



- 1 Quantifying new versus old aerosol deposition in forest canopies: new throughfall mass balance with
- 2 fallout radionuclide chronometry
- 3 Joshua D. Landis¹
- ¹Dartmouth College, 19 Fayerweather Hill Road, Hanover NH 03755 USA
- 5 correspondence to joshua.d.landis@dartmouth.edu

7 Abstract

6

8

9

10

11

12

13

14

15

16

17

18

19

20 21

22

23

24

25

26

27

28

Net throughfall (NTF) measurements of the fallout radionuclides (FRNs) ⁷Be and ²¹⁰Pb confirm that precipitation is a strong net source of secondary aerosol and particulate matter (PM) to a temperate forest canopy, which retains nearly 60% of total wet and dry annual atmospheric flux of the FRNs (four trees, three species, two sites, n=159). Estimation of dry deposition using a multiple regression technique and predictors of precipitation depth and duration of the antecedent dry period agrees well with ecosystem mass balance, with about 25% of both ⁷Be and ²¹⁰Pb annual flux deposited by dry processes, and total FRN fluxes in reasonable agreement with regional soil inventories. In contrast to the FRNs, other trace metals (TMs) including Pb and Hg show large enrichments in throughfall which derive from processes of internal ecosystem recycling including PM resuspension, leaching from tree metabolic pathways, and physicochemical weathering of non-foliar biological tissues of the tree canopy (collectively 'phyllosphere'). To estimate the contributions to net throughfall from these internal pathways, which we term a change storage (ΔS), a new FRN canopy mass balance is derived based on the different half-lives of ${}^{7}\text{Be}$ and ${}^{210}\text{Pb}$. Estimated ΔS for selected elements are: $SO_4=7\%$; ${}^{210}\text{Pb}=29\%$; As =42%; ${}^{9}Be=45\%$; Cd =60%; Hg =60%; Pb =63%; Fe =79%; Al =79%; P =91%. The balance of throughfall (1-ΔS) represents new ecosystem inputs. Change in storage for all elements was strongly correlated with export of particulate carbon (FPOM) and dissolved organic carbon (DOC) from the canopy, indicating that PM transformation during residence within the canopy facilitates metal release from storage. ΔS thus represents an emergent ecosystem property through which metal, carbon, and hydrologic cycles converge to determine the fate, reactivity, and timing of metal delivery to underlying soils. The forest canopy represents a substantial reservoir of decadally-aged PM and cannot be assumed at steady-state with respect to ongoing atmospheric deposition, especially in the context of changing atmospheric composition, e.g., declining industrial emissions of Pb and Hg.

293031

Plain Language Summary

- 32 Particulate matter (PM) in the atmosphere contains nutrients and toxins that impact the health of both
- 33 humans and ecosystems. Understanding how PM is deposited to land from the atmosphere is
- 34 challenging, however, due to its very small size and complex composition. Here we develop a new
- 35 method using natural radioactive elements to better measure how much PM is deposited, well as the
- timescales over which it recirculates between the atmosphere and land.





1. Introduction

biosphere interactions.

Forest vegetation covers over 30% of the earth's landmass and thus mediates the impacts of particulate matter (PM) deposition on climate, ecosystem function, and human health (Bortolazzi et al., 2021; Emerson et al., 2020; Farmer et al., 2021; Hosker and Lindberg, 1982; IPCC, 2021; Jiskra et al., 2018; Johnson and Siccama, 1983; Lindberg et al., 1982; Lovett and Lindberg, 1984; McDowell et al., 2020; Van Stan and Pypker, 2015; WHO, 2016, 2021). Despite regulating the composition of both the atmosphere and terrestrial ecosystems, however, the PM-vegetation interaction remains poorly understood. Even a basic understanding of mechanisms that regulate PM uptake by vegetation remain elusive (Luo et al., 2019; Shahid et al., 2017; Zhou et al., 2021). As a result, in part, current estimates for PM dry deposition in global chemical transport models vary across orders of magnitude, underpredict direct observations by as much as 200%, omit fundamental processes such as resuspension, and lack verification by mass balance (Emerson et al., 2020; Farmer et al., 2021; Hicks et al., 2016; Pryor et al., 2017; Saylor et al., 2019). Moreover, long residence times of PM in recirculation at the earth surface prolong impacts of critical pollutants such as Hg and Pb, and their ultimate fate remains unclear (Resongles et al., 2021; Wang et al., 2020). These uncertainties underscore a critical need for improved understanding of PM-

Two approaches are used for measuring PM deposition to forest canopies, each with characteristic advantages and limitations (e.g., Draaijers et al., 1996). Micrometeorological approaches infer rates of PM deposition based on aerosol concentration gradients in air, or covariance of airborne concentrations with turbulence (e.g., eddy flux; Emerson et al., 2018; Laguionie et al., 2014; Obrist et al., 2021). These methods are critical insofar as they estimate PM deposition over large areas and in some cases with resolution PM sizes, but results are dependent on assumptions regarding micrometeorological physics, do not provide information on PM composition, and ultimately lack verification by mass balance ("where did it go?"). A complementary approach exploits canopy chemical mass balance, comparing precipitation collected under vegetated canopies (throughfall or TF) with paired bulk deposition measurements under open sky (openfall or OF). Positive net throughfall (NTF = TF- OF) results for most elements. The excess is conventionally attributed to some combination of washoff of dry deposition that has accumulated in the canopy during the preceding dry period and leaching/weathering from biological tissues of the canopy itself. No accommodation is made for long-term PM storage in ecosystem components, however, and quantifying the contribution of dry deposition thus requires uncertain assumptions for distinguishing between these competing processes ("where did it come from?"; Lovett & Lindberg, 1984; Ulrich, 1983). Distinguishing these processes is critical for understanding ecosystem trace metal budgets, since they can represent either a novel external source via dry deposition of PM, or internal recycling via resuspended dust or leaching of biological materials (Avila and Rodrigo, 2004; Lindberg et al., 1982).

One critical source of error in throughfall mass balance is the assumption that precipitation is a simple and efficient process of 'washoff' that fully removes PM dry deposition that has accumulated during dry periods preceding the rain event (Bishop et al., 2020; Gandois et al., 2010; IAEA, 2009; Lovett and Lindberg, 1984; USEPA, 2005). The canopy is thus assumed at steady-state, and no accommodation is made for accumulation of PM over time, or for any change in storage within the canopy. Support for precipitation as an efficient washoff process derives from the large enrichments of most elements that are observed in throughfall, experimental dry applications of PM to vegetation which show residence times on the order of just days to weeks (Chamberlain, 1970; Miller and Hoffman, 1983), and washing of natural vegetation which shows exponential declines in rates of metal extraction (Avila and Rodrigo, 2004; Shanley, 1989). This conceptualization of washoff also aligns with the 'Lotus effect', which is the





82 efficient self-cleaning of leaves by raindrops due to their hydrophobic waxy cuticle (Barthlott and 83 Neinhuis, 1997). 84 On the other hand, it is well documented that a range of atmospheric metals and metalloids accumulate 85 continuously in vegetation during exposure to the atmosphere. These include the natural fallout radionuclides (FRNs) ⁷Be and ²¹⁰Pb (Landis et al., 2014; Sumerling, 1984), anthropogenic fission products 86 including ⁹⁰Sr (Yamagata et al., 1969), ¹³¹I (Yamagata, 1963), ¹³⁷Cs and others (Kato et al., 2012; Russell et 87 al., 1981), trace metals (TMs) including Al, Pb and Hg (Landis, 2024a; Rea et al., 2001, 2002; Wyttenbach 88 89 and Tobler, 1988), and oxoanions AsO₃, SeO₃ and CrO₄ (Landre et al., 2009). Moreover, this 90 accumulation continues unabated in senescent vegetation, indicating that PM uptake is independent of 91 leaf physiology and thus unambiguously atmospheric in origin. The foliar metal residence times of Hg, ⁷Be, ²¹⁰Pb, and ¹³⁷Cs have been shown by various means to exceed 700 days, which is generally longer 92 93 than the lifetime of the foliage itself. This demonstrates strong coupling of PM metals to the carbon 94 cycle (Graydon et al., 2009; Kato et al., 2012; Landis et al., 2014). In the case of Hg, recent 95 measurements show that long-lived non-foliar materials of the forest canopy including bark, lichen, 96 moss, and foliage (collectively "phyllosphere") collectively retain many times the annual Hg flux on an 97 areal basis (Wang et al., 2020). This demonstrates both long residence times for PM metals in the 98 phyllosphere, and that surfaces other than foliage may play a dominant role in canopy and ecosystem 99 mass balances (Obrist et al., 2021). Further, stable isotopes of both Hg and Pb reveal that legacy 100 anthropogenic emissions continue to dominate contemporary atmospheric deposition despite large 101 reductions in both emissions and measured rates of deposition (Farmer et al., 2010; Resongles et al., 102 2021; Taylor et al., 2022; Yang and Appleby, 2016). Resolving multiple processes that regulate PM 103 accumulation, storage, and re-suspension in terrestrial ecosystems, and their contributions to PM 104 depositional budgets, remains a challenge to biogeochemical research. This is especially important in the 105 context of changing global emissions of, e.g., Hg and Pb, since the forest cannot be assumed at steady-106 state with respect to contemporary deposition. The natural fallout radionuclide (FRN) tracers ⁷Be and ²¹⁰Pb provide a novel and emerging perspective on 107 108 PM metal cycling. The FRNs have been shown to accumulate in vegetation primarily by wet deposition 109 rather than dry as widely presumed (Landis, 2024a; Landis et al., 2014). This distinction is important because approximately 90% of PM removal from the atmosphere occurs by wet processes (in 110 111 continental climates), and the accumulation of FRNs in forest canopies might thus reflect a quantitative 112 view of PM cycling from the atmosphere. The FRNs ⁷Be and ²¹⁰Pb are secondary aerosols produced in 113 the atmosphere from gaseous precursors by cosmogenic spallation of N2 and O2 or radiogenic decay of 114 ²²²Rn, respectively, with identical PM activity-size distributions (mean aerodynamic diameters) of ca. 0.5 115 μm (Gründel and Porstendörfer, 2004; Winkler et al., 1998). FRNs are widely exploited as tracers of 116 other PM components of broad interest including PM2.5, black carbon, sulfate, and anthropogenic trace 117 metals in long-range transport (Koch et al., 1996; Lamborg et al., 2013; Landis et al., 2021a; Liu et al., 118 2016). 119 The FRNs hold special power as PM tracers through two consequences of their radioactive decay. First, 120 their accumulation in the terrestrial environment is limited such that their occurrence can be 121 unambiguously traced directly to an atmospheric origin. Second, their characteristic rates of decay can 122 be exploited to explicitly measure timescales of their deposition and redistribution. For example, ⁷Be and ²¹⁰Pb are produced in the atmosphere with a typical activity ratio on the order of 10. In vegetation 123 124 exposed to ongoing atmospheric deposition, both FRNs accumulate with time but the ⁷Be:²¹⁰Pb ratio 125 decreases due to their differing half-lives. After one year of exposure foliage has ratios of 2-3. With its 126 short half-life of 54 days, ⁷Be records the PM-vegetation interaction over event-based timescales,





- whereas ²¹⁰Pb records longer-term storage, resuspension, and recycling of PM deposition over
- subannual to decadal timescales (Landis et al., 2021a; Landis et al., 2021b) .
- 129 Here we use FRN chronometry in a new throughfall mass balance approach to resolve processes and
- timescales that govern PM deposition and interaction with forest canopies. We first review
- 131 contemporary approaches to throughfall mass balance and then derive a new expression using FRNs to
- distinguish the initial absorption of PM during deposition from later release from canopy storage. We
- confirm that ⁷Be and ²¹⁰Pb are not systematically fractionated and that the ⁷Be:²¹⁰Pb ratio in throughfall
- 134 is primarily a measure of PM age. We then extend our throughfall mass balance approach to link the
- 135 FRNs and MTEs to canopy export of dissolved organic carbon (DOC) and fine particulate organic matter
- 136 (FPOM).

1.1. Throughfall mass balance

- 138 The conventional throughfall mass balance includes two pathways by which PM enters and leaves the
- 139 canopy. Inputs to the canopy by bulk wet deposition (W) or dry deposition (D) must be balanced by
- 140 exports via wet throughfall (*T*) and any exchange with the canopy (*C*) via leaching (+) or absorption (-):

141
$$W + D = T \pm C$$
 Eq. 1

- 142 Bulk deposition (W) is measured under open sky adjacent to the forest where it may also be called
- openfall (OF). Net throughfall (NTF) is the arithmetic difference between deposition under the canopy
- 144 and open sky:

145
$$NTF = T - W = D \pm C$$
 Eq. 2

- W and T are easily measured. The challenge in estimating D by mass balance then remains to distinguish
- 147 contributions of C. Two approaches have been proposed. The more common is the 'filtering' approach
- 148 (Staelens et al., 2008; Ulrich, 1983; Yoshida and Ichikuni, 1989) where an index element is used to
- apportion dry deposition of the target element, D_i . The index element, typically Na or Al, is assumed to
- 150 have identical rates of dry deposition as the target element (Eq. 3) but no metabolic contribution from
- the canopy. This assumption implicitly presumes similar PM size distributions, and thus sources with
- respect to secondary or primary emission, insofar as PM size controls rates of dry deposition (Jaenicke,
- 153 1980).

$$\frac{D_i}{W_i} = \frac{D_{Na}}{W_{Na}}$$
 Eq. 3

155 With C_{Na} =0, dry deposition of an element of interest can be calculated as follows:

156
$$D_i = W_i \cdot \frac{T_{Na} - W_{Na}}{W_{Na}} = W_i \cdot (EF_{Na} - 1)$$
 Eq. 4

- Here, EF_{Na} represents the Na enrichment factor =T/W. Following the calculation of D_i by Eq. 4, C_i can be
- solved from Eq. 2. By this approach any EF_i greater than EF_{Na} yields a positive C_i , which represents
- leaching from the canopy. Any EF_i less than EF_{Na} yields negative C_i , which represents a net loss to the
- 160 canopy by absorption.
- 161 A second approach to describing the canopy interaction uses multiple regression of individual storm
- 162 events to estimate rate constants for specific canopy processes (Lovett and Lindberg, 1984; Rea et al.,
- 163 2001; Wu et al., 1992):

164
$$NTF = T - W = D + C = \beta_1 A + \beta_2 P$$
 Eq. 5





- 165 The coefficient β_1 represents the rate of dry deposition to the canopy [Bq m⁻² d⁻¹ or μ g m⁻² d⁻¹] and A is
- the duration of the antecedent dry period preceding the storm event [days]. The coefficient β_2
- 167 represents either canopy leaching or absorption [Bq or µg m⁻² cm⁻¹] with P the precipitation total [cm].
- 168 Biotic leaching and abiotic exchange (desorption, dissolution) can be distinguished only by a priori
- 169 assumptions based on elemental chemistry, and that one must dominate the other, for example that
- 170 base cations K, Ca, Mg, etc., are strongly cycled through leaf tissue and are thus derived primarily from
- 171 leaching, whereas trace metals, e.g. Pb, are not appreciably cycled and are thus dominated by canopy
- 172 exchange (Lovett and Lindberg, 1984).
- 173 An important advantage to this approach is that, provided sufficient measurements, additional
- 174 explanators might be added to the multiple regression to understand effects from other environmental
- 175 factors such as seasonality, tree species, precipitation pH, dissolved organic carbon (DOC), or fine
- 176 particulate organic matter (FPOM).

1.2. FRN mass balance: change in canopy storage

- 178 The observed accumulation of FRNs and TMs in foliage and long-lived tissues of the phyllosphere
- 179 requires that canopy exchange must accommodate a change in storage, if previously deposited PM is
- 180 later susceptible to weathering processes and export from the canopy in subsequent rainfall over some
- 181 characteristic timeframe. We can distinguish this change in storage as a separate term in mass balance
- as follows based on their different characteristic timescales:

183
$$T = W + D \pm (C + \Delta S)$$
 Eq. 6

- 184 Analogous to the use of an index element for dry deposition in the filtering approach, we propose to use
- 185 ⁷Be as an index of canopy storage. Beryllium is highly reactive to natural surfaces but due to its short
- half-life, ⁷Be cannot record long-term storage. In contrast, the longer-lived ²¹⁰Pb persists to record PM
- 187 fate over annual to decadal timescales. The similar occurrence and behaviors of ⁷Be and ²¹⁰Pb, but
- different half-lives, thus allow us to distinguish instantaneous canopy exchange (sorption or leaching)
- 189 from a subsequent change in storage. Storage is thus defined as occurring over timescales that are long
- 190 relative to the 7 Be half-life (54 days). We write two equations to solve for one unknown, ΔS :

191
$$T_{Be} = W_{Be} + D_{Be} \pm C_{Be}$$
 Eq. 7

192
$$T_{Ph} = W_{Ph} + D_{Ph} \pm (C_{Ph} + \Delta S)$$
 Eq. 8

- 193 Eq. 7 ignores radioactive decay, with an assumption that the residence time of dry deposition in the
- 194 canopy is very short (days) relative to the ⁷Be half-life. This assumption is re-evaluated in *Sect. 3.4*. Based
- on their congruent interactions with natural vegetation and particulate matter (Landis, 2023; Landis et
- al., 2014, 2016, 2021b, 2024a), we next assume that ⁷Be and ²¹⁰Pb have similar canopy interactions and
- that for both C is an equivalent fraction of total wet+dry deposition (Eq. 9).

$$\frac{c_{Be}}{W_{Be}EF_{Na}} = \frac{c_{Pb}}{W_{Pb}EF_{Na}}$$
 Eq. 9

199 This allows us to combine Eq. 7 and Eq. 8, with both D and C terms cancelling. We then solve for ΔS as 200 follows, by which we attribute any throughfall excess in 210 Pb relative to 7 Be to a change in storage:

$$\Delta S = T_{Pb} - T_{Be} \cdot \frac{w_{Pb}}{w_{Be}} \tag{Eq. 10}$$

- 202 For cases of aerosols with a gaseous phase such as Hg or SO_4 , we cannot assume a constant D/W ratio as
- 203 in Eq. 3. In these cases, we use an alternative mass balance by directly estimating dry deposition via
- multiple regression (θ_1) for both ⁷Be and, e.g., Hg, as follows:





 $\Delta S_{Hg} = Hg_{NTF*} - Be_{NTF*} \cdot \frac{W_{Hg} + D_{Hg}}{W_{Be} + D_{Be}}$ Eq. 11

- The term Hg_{NTF^*} represents NTF without contribution from C, i.e., $Hg_{NTF^*} = T_{Hq^-} W_{Hq^-} D_{Hq}$.
- 207 Finally, calculating a change in storage acknowledges that a process of exchange occurs within the
- 208 canopy. Some fraction of new wet and dry deposition is retained by the canopy, while some fraction of
- 209 previous deposition is released from storage. The proposed mass balance thus provides a new
- 210 perspective on aerosol deposition, new versus old. ΔS quantifies the old, and the fraction new is follows
- 211 from mass balance:

$$Hg_{new} = T_{Hg} - Hg_{\Delta S}$$
 Eq. 12

213 2. Methods

214

215

2.1. Site and tree characteristics

- We measured 156 samples of throughfall under mature canopies of two tree species at each of two
- 216 sites. The Beaver Meadow (BM) site in Sharon, Vermont (104 km², population =1500) sits at an elevation
- 217 of 502 m in mixed forest of sugar maple, red oak, American beech, white pine, and poplar, with
- 218 understory of striped maple and hornbeam. Annual precipitation averages 117 cm y⁻¹ for the past 30
- 219 years (PRISM Climate Group, Oregon State University, https://prism.oregonstate.edu, data created 4
- 220 Feb 2014). The site is underlain by green schists of the Waits River series and thin glacial till which leads
- 221 to development of well-drained soils typically classified as Inceptisol. Throughfall was collected under
- red oak (Quercus rubra; diameter at breast height, dbh =28 cm) and white pine (Pinus strobus; dbh = 59
- cm) in the forest interior, and openfall was collected within 50 m in an adjacent forest gap. The Shattuck
- Observatory (SO) site is located 18 km distant in Hanover, New Hampshire (130 km², population =8500),
- in the semi-urban forest of the Dartmouth College Park at an elevation of 165 m. Annual precipitation
- averages 101 cm y⁻¹ (PRISM Climate Group, Oregon State University, https://prism.oregonstate.edu,
- 227 data created 4 Feb 2014). The SO site is underlain by mafic volcanics of the Ammonoosuc series with
- 228 frequent outcrops along this ridgeline site (Schumacher, 1988). Throughfall was collected under red oak
- 229 (dbh = 53 cm) and Norway spruce (*Picea abies*; dbh = 60 cm) at the forest edge, with openfall collected
- 230 within 50 m in the adjacent clearing where we have previously reported a long-term timeseries of
- atmospheric deposition Landis et al., 2021a; Landis et al., 2021b).
- 232 The sampled trees represent a range of foliar ages and characteristics that may influence FRN activities
- and MTE concentrations. Red oak is deciduous and sheds most leaves annually after ca. 6 months of
- 234 growth (May-October); however, some remain on branches following abscission through the following
- winter (a phenomenon called marcescence). White pine retains needles for 1.5-2 years. Norway spruce
- retains needles for up to 5-8 years (Reich et al., 1996). Leaf area index (LAI) at each throughfall site was
- estimated over a 30° zenith angle using hemispheric photos and the software package Hemisfer
- 238 (Schleppi et al., 2007; Thimonier et al., 2010). Measured LAI are as follows: BM oak (leaf off) =0.9 ±0.3,
- 239 BM oak (leaf on) = 3.1 ± 0.5 , BM pine = 2.79 ± 0.14 , SO oak (leaf off) 1.13 ± 0.4 , SO oak (leaf on) = 5.9 ± 0.6 ,
- 240 SO spruce =4.52 ±0.16.

241

2.2 Sample collection and filtration

- 242 Each openfall and throughfall precipitation sampler consisted of 4 tandem polyethylene open collectors
- 243 (area =650 cm² each, depth=40 cm; cumulative projected area = 0.26 m²) mounted to a PVC post at a
- 244 height of 1.5 m above ground. Total collector surface area to projected ground area (surface area index)
- 245 =5.2 (e.g., Hicks, 1986). At each site samplers were located at the same aspect relative to the sampled
- 246 tree stem, under the midpoint of the tree crown to avoid dripline or stem effects. Collectors were





247 deployed prior to, and retrieved following, individual rain and snowstorms. Upon retrieval an aliquot 248 was immediately removed for measurement of operationally-dissolved MTEs and DOC. This aliquot (a0) 249 was filtered with a 0.45 µm Nylon filter (Fisher Scientific), the first 1 mL discarded, and next 5 mL used to 250 rinse an acid-washed polyethylene vial and discarded, and a final 20 mL retained and acidified to 2% HCl 251 (Optima grade). Sample pH was then measured in the bulk sample with dual ROSS-type electrodes 252 (Thermo Scientific), calibrated daily with fresh, low ionic strength buffer. Bulk samples were then passed 253 through a 1 mm polypropylene screen or hand-picked to remove coarse debris and then filtered to tared 254 0.5 µm quartz fiber filters (QFF; Advantech QR-100) to remove an insoluble fine particulate organic 255 fraction (FPOM). The filtrate was acidified to 2% HCl with concentrated acid (Trace Metal grade), and the 256 acidified sample in turn was used to rinse and recover metals absorbed to the sample collection train 257 and collector surfaces.

FPOM on QFF filters was extracted sequentially using 2% HCl and reverse aqua regia (9:3 HNO₃:HCl, plus 0.2 mL BrCl) to estimate MTE solubility and distinguish fluxes of dissolved (*d*.Pb, etc.), soluble, and total aerosol deposition. The acid-soluble fraction (*s*.Pb, etc.) is the sum of dissolved and 2% HCl extraction. The total fraction (*t*.Pb, etc.) is the sum of dissolved, 2% HCl, and aqua regia fractions. The acid soluble fraction is considered environmentally relevant (Lindberg and Harriss, 1981; Mahowald et al., 2018).

From dissolved and FPOM fractions we calculated distribution coefficients (K_D) as follows, where V is total sample volume (mL) and M is FPOM mass (g):

265
$$K_D = \frac{d.Pb/V}{(t.Pb-d.Pb)/M}$$
 Eq. 13

Enrichment factors of MTEs with respect to upper continental crust (EF_{crustal}) were calculated from dissolved fractions in OF collections to maintain comparability the prior works (Duce et al., 1975; Gandois et al., 2010; Taylor and McLennan, 1995):

$$EF_{crust} = (M_i/Al)_{OF}/(M_i/Al)_{crust}$$
 Eq. 14

2.3. Sample Analysis

269

270

285

286

287

288

271 FRNs were measured by gamma spectrometry following preconcentration by MnO₂ co-precipitation, 272 with yields averaging 88 ±15% for Be and 88 ±16% for Pb (mean ±SD). Details are given elsewhere 273 (Landis et al., 2012, 2021). MTEs were measured by inductively-coupled plasma optical emission 274 spectrometry (ICPOES; Spectro ARCOS) operated in axial view. Low-level trace elements including As, Cd, 275 Co, Cr, Cu, Fe, Pb, and V were measured by ICP triple-quadrupole mass spectrometry (ICPMS-QQQ; 276 Agilent 8900) in the Dartmouth Trace Element Analysis Core Facility (TEA Core). Reference material 277 NIST1643f was used for quality control, with recoveries within 95-105% for all analytes. Total Hg was 278 measured by double amalgamation purge-and-trap atomic fluorescence (Brooks Rand Merkx-T, Model 279 III), where samples preserved in 2% HCl were oxidized by reaction with 1% v/v BrCl at room temperature 280 for 24 hours and then reduced to Hg₀ by addition of SnCl₂ and hydroxylamine immediately prior to 281 analysis. Reference material NIST1641e was used for Hg quality control, with recovery of 10 pg 282 averaging 97 ±8% (mean ±SD; n=48). Sample recovery spikes averaged 97 ±6% (n=9). Dissolved organic 283 carbon (DOC) was measured by automated combustion of acidified samples (General Electric); see also 284 Hou et al. (2005) and Gandois et al. (2010).

2.4. Statistical analyses

Statistical analyses were performed in JMP Pro 16.0. Data were transformed to achieve normal distributions and equal variances. For NTF which includes positive and negative values, this required transform of the form $log_{10}(x+n)$ with n selected to scale all values >0. Our multiple regression approach





is described in more detail elsewhere (Landis et al., 2021a). We observe Bonferroni correction for describing significance of multiple regression parameters but presented *p*-values do not include this correction since the number of explanators are shown for each regression.

2.5. Literature review

Throughfall enrichment factors were compiled from the following literature sources (Ali et al., 2011; Atteia and Dambrine, 1993; Avila and Rodrigo, 2004; Böhlke and Michel, 2009; Bringmark et al., 2013; Demers et al., 2007; Eisalou et al., 2013; Forti et al., 2005; Fu et al., 2010; Gandois et al., 2010; Graydon et al., 2008; Grigal et al., 2000; Henderson et al., 1977; Hou et al., 2005; Huang et al., 2011; Iverfeldt, 1991; Karwan et al., 2016, 2018; Kolka et al., 1999; Kopáček et al., 2009; Landre et al., 2009; Larssen et al., 2008; Lawson and Mason, 2001; Lindberg and Harriss, 1981; St. Louis et al., 2001, 2019; Mahendrappa, 1987; Małek and Astel, 2008; Matschullat et al., 2000; Michopoulos et al., 2005, 2018; Oziegbe et al., 2011; Petty and Lindberg, 1990; Rea et al., 2001; Rehmus et al., 2017; Rodrigo et al., 1999; Schwesig and Matzner, 2000; Skrivan et al., 1995; Sohrt et al., 2019; Stachurski and Zimka, 2000; Tan et al., 2019; Ukonmaanaho et al., 2001; Wang et al., 2020; Wilcke et al., 2017; Zhang and Liang, 2012).

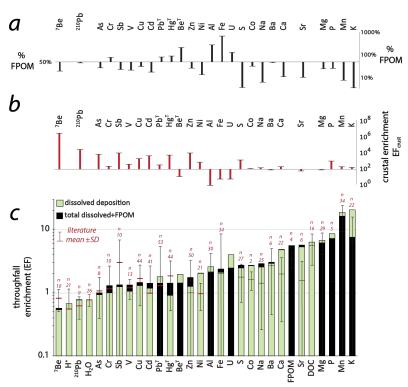


Figure 1. throughfall enrichment factors for FRNs and MTEs. (a) % increase in throughfall flux when including a fraction extracted from fine particulate organic matter (FPOM); (b) crustal enrichment factors, where $EF_{crustal} = [M/Al]_{OF}/[M/Al]_{crust}$. (c) Median flux-based throughfall enrichment factors (EFs) for this study shown in bars. Note log_{10} scaling. Line and whiskers show means and standard deviations compiled from literature sources, with number of experiments indicated as n (see *Methods*).



313

346



3. Results

3.1. FRN mass balance in the forest canopy

- Throughfall enrichment factors and the partitioning of FRNs and MTEs to FPOM are shown in Fig. 1.
- 315 Throughfall measurements including rainfall interception, FPOM, and DOC concentrations are shown in
- 316 Fig. S1. The studied tree canopies typically intercept (retain) 20% of precipitation. DOC and FPOM are
- 317 greatly increased through the canopy with TF concentrations in ranges of 1-10 µg mL⁻¹ and 10-100 µg
- 318 mL⁻¹, respectively. Throughfall mean pH values for the seasons summer through winter were 5.29, 5.36,
- 319 4.98, and 4.86, respectively. Effect of the canopy on throughfall pH was variable (Fig. S2). The canopy
- 320 was a net sink for H^+ in summer for each of spruce, pine, and oak [p<0.05]. On an annual basis, oak was
- a net sink at both sites but both pine and spruce were net sources of H⁺.
- 322 Flux-based throughfall enrichment factors (EFs) for ⁷Be and ²¹⁰Pb were 54.7 ±0.3% and 75.9 ±1%,
- 323 respectively (±SE), significantly lower than 1 and thereby demonstrating that the canopy is an
- 324 unambiguous net sink for FRNs in wet deposition. ⁷Be shows stronger absorption than either H⁺ or H₂0,
- which demonstrates its strong preferential absorption by the canopy. Only the following showed EFs
- 326 less than 1: 7 Be < H $^{+}$ < 210 Pb < H $_{2}$ O < As. All other MTEs showed a net gain through the canopy due to
- 327 some combination of dry deposition during the antecedent dry period, leaching from biological tissues,
- or weathering from storage in the phyllophere. Putative reference elements expected to have minor
- leaching contributions such as Al, Fe, U and Na showed moderate gains from the canopy, with EFs in the
- 330 range of 2-3. The following trace metals showed EFs less than these reference elements, which
- 331 nominally indicates net sorption to the canopy: Cr, Sb, V, Cu, Cd, Pb, Hg, 9Be, Ni and Zn. Alkaline and
- 332 nutrient elements showed much larger EFs than reference elements, indicating strong net gains from
- the canopy: Co, Ba, S, Ca, Sr, Mg, P, C, Mn and K, as well as DOC and FPOM.
- 334 Crustal enrichment factors (EF_{crust}) in the range of 10²-10³ indicate that PM metals are generally of
- 335 anthropogenic atmospheric origin, whereas values ~1 confirm a terrestrial dust source for Al, Fe, and U
- 336 (Duce et al., 1975; Fig. 1b). EFcrust does not strictly identify atmospheric PM however, since values in the
- 337 range of 10² for alkaline elements can also reflect the high solubility of these elements and their
- extraction from biological tissues of the phyllosphere during rainfall.
- Among tree species, spruce displayed lowest EFs for ⁷Be and ²¹⁰Pb (highest interception), but higher EFs
- than either oak or pine for most elements [p<0.05]. By site, both spruce and oak at the SO site showed
- 341 higher EFs for 9Be, Ni, Sb, V and Zn, demonstrating a site effect for these elements which could be
- 342 related to higher pollutant loads near a higher population density, or alternatively to underlying mafic
- 343 lithology at this site [p<0.05]. By contrast, there were no species or site effects for the heavily cycled
- elements Ca, Mg, K, P or Mn, or for metals including Cd, Cu, Hg, Pb, or U [p>0.05]. Tree species were
- 345 compared only during deciduous leaf-on months.

3.2. Interpreting canopy processes from FRN throughfall concentrations

- 347 Throughfall EFs evaluated on an annual basis described above show that the FRNs sorb strongly and that
- 348 the canopy is therefore a strong sink for secondary aerosol metals. For further insights into the balance
- 349 of processes acting to retain and release FRNs within the canopy at the event-scale, we also evaluated
- 350 the concentrations of FRNs as a function of precipitation depth for individual storms. Below 2 cm of
- 351 precipitation both ⁷Be and ²¹⁰Pb concentrations in TF are generally greater than 100% of concentrations
- 352 in OF, and in some cases more than 300% higher than incident precipitation. This indicates that net
- 353 release of FRNs is the dominant process at low precipitation totals, which we attribute to the removal of
- dry-deposited aerosol which were deposited during the antecedent dry period (Fig. 2a).





Beyond 2 cm of precipitation the concentrations of both ⁷Be and ²¹⁰Pb are lower than openfall, indicating that the canopy transitions to a net sink with increasing precipitation depth. This suggests that at some threshold amount of precipitation, susceptible dry-deposited aerosol is fully removed, and wet deposited aerosols continue to be absorbed by the canopy. The unambiguous net sorption of wet-deposited aerosols is clear when concentrations are converted to fluxes (by multiplication with precipitation depth; Fig. 2b). At highest precipitation totals >6 cm there is some suggestion that sorption capacity of the canopy may be exhausted and FRN yields from the canopy begin to increase, but data are too few for a clear interpretation.

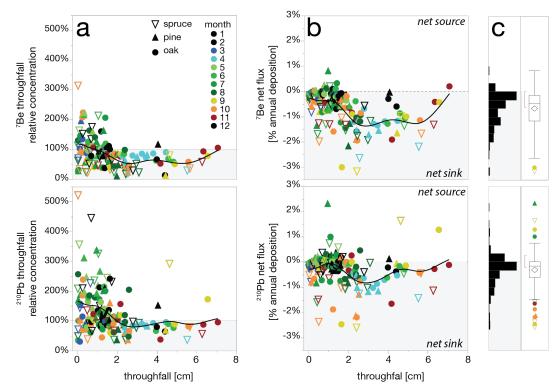


Figure 2. relative concentrations of ⁷Be or ²¹⁰Pb in throughfall versus openfall (EF=TF/OF). (a) Oak is shown with circles, pine with triangles, spruce with open triangles. Black lines show a spline best-fit. (b) net throughfall fluxes (NTF) of ⁷Be and ²¹⁰Pb as a percentage of total annual deposition. (c) histograms of ⁷Be and ²¹⁰Pb net flux.

3.3. Throughfall ⁷Be:²¹⁰Pb ratios as a metric of PM age

²¹⁰Pb is systematically biased to higher yields than ⁷Be despite the same patterns in canopy interactions, and as a result ⁷Be:²¹⁰Pb ratios are significantly lower in throughfall versus openfall (Fig. 2a, Fig. S2). Mean throughfall ⁷Be:²¹⁰Pb ratios across all species averaged 10.3 ±0.3 versus mean openfall of 14.8 ±0.5 [mean ±SE]. Throughfall for each tree species was significantly lower than paired openfall measurements [p<0.0001]. There was no correlation between throughfall pH and the ⁷Be:²¹⁰Pb ratio that might indicate discrimination of the FRNs through aqueous chemistry [R²=0.001, p=0.80; Fig. S2b]. We next used multiple regression to identify independent explanators on throughfall ⁷Be:²¹⁰Pb ratios and to quantify their independent effects on ⁷Be:²¹⁰Pb; we report independent effects as the % of total variance



406

407

408

409

410

411

412



explained by each variable [in brackets] (Fig. S3). A predictive model for ⁷Be:²¹⁰Pb showed these 377 significant explanators: species [22%], season [12%], and ⁷Be:²¹⁰Pb ratio of incident precipitation [9%] 378 [R²= 0.42]. Adjusted for season and incident ratio, ⁷Be:²¹⁰Pb ratios among species increased in order: 379 spruce $(7.9 \pm 0.6)^A$ < pine < $(9.5 \pm 0.6)^B$ oak $(11.9 \pm 0.5)^C$. Adjusted for both species and incident ratio, 380 seasonal ratios increased in order: autumn $(7.6)^A$ < summer $(9.9)^B$ < winter $(10.5)^{BC}$ < spring $(11.3)^C$. Both 381 382 species and seasonal patterns are consistent with the impact of tree phenology on long-term storage of ²¹⁰Pb, with the higher LAI and older foliage of conifers storing larger reservoirs of ²¹⁰Pb, which is 383 384 exported in small amounts during subsequent storms.

The strongest discrimination between ⁷Be and ²¹⁰Pb appears to be their characteristic half-lives, in 385 absence of any evidence for impacts by environmental factors. There was no effect on ⁷Be:²¹⁰Pb from 386 antecedent dry period [R²=0.01, p=0.27], suggesting no discrimination in dry deposition between ⁷Be 387 388 and ²¹⁰Pb. There was no positive correlation between rainfall depth and ⁷Be:²¹⁰Pb [R²=0.03, p=0.42], in 389 contrast to OF where a strong positive correlation reflects the washout-rainout transition (Landis et al., 390 2021). Importantly, there were no significant effects from factors that might indicate discrimination 391 between Be and Pb aqueous chemistries including: pH [p=0.32], $log_{10}(K_D)$ for either ⁷Be [p=0.34] or ²¹⁰Pb 392 [p=0.18], FPOM [p=0.29], DOC [p=0.47], or any MTE concentrations, fluxes, net fluxes, or enrichment 393 factors [p>0.05].

3.4. Multiple-regression mass balance to quantify dry deposition

395 We used multiple-regression mass balance to quantify the independent influences of wet and dry 396 deposition and canopy interactions that determine net throughfall (NTF) of the FRNs (Eq. 5). Overall model fits for NTF are good for both 7 Be [R²=0.49, p<0.0001] and for 210 Pb [R²=0.30, p<0.0001] (Fig. 3). 397 398 Both ⁷Be and ²¹⁰Pb show positive effects with antecedent dry period (θ_1) [p<0.05], and inverse effects 399 from precipitation depth (θ_2) apparent from Fig. 2 [p<0.05]. For ⁷Be the dry deposition rate (θ_1) is 400 equivalent to 213 ±53 Bg m⁻² per year or 13 ±4% of total annual deposition, assuming that all dry 401 deposition is fully removed by subsequent storms. The multiple regression dry deposition estimate does 402 not incorporate ⁷Be decay that occurs during the antecedent period. However, with a decay rate of 1.3% 403 per day, and median antecedent period of 7 days (mode of 2 days), underestimation of ⁷Be dry 404 deposition by ignoring radioactive decay is likely <10% of estimated dry deposition or <20 Bq m⁻² y⁻¹). For 405 ²¹⁰Pb, θ_1 is equivalent to 19 ±6 Bq m⁻² per year or 15 ±5% of total annual deposition.

It is important to observe from Fig. 2 that dry deposition is not fully removed from the canopy by subsequent rainfall since FRN concentrations may be higher in throughfall versus incident precipitation for up to 2 cm of precipitation. During and following rain events it is thus likely that a complex exchange is occurring at the leaf surface between wet and dry deposited PM, and both components are likely to be absorbed by the leaf especially at low rainfall totals. In this case the multiple regression estimate of dry deposition is underestimated by a factor equal to the efficiency with which dry deposition is absorbed by the canopy. Implications for dry deposition absorption are discussed below in *Sect. 4.1*.

Dry deposition to the canopy is likely derived from ambient PM and not from resuspension of dust. The 7 Be: 210 Pb ratio of dry deposition to the canopy based on multiple regression coefficients =11 ±4, which is comparable to our prior measurements of ambient PM10 (=10 ±2), and somewhat lower than openfall wet deposition [flux-weighted average = 15.1 ±0.6; p=0.22], but significantly higher than bulk dry deposition [=4.2 ±0.6, p<0.0001] (Landis et al., 2021).





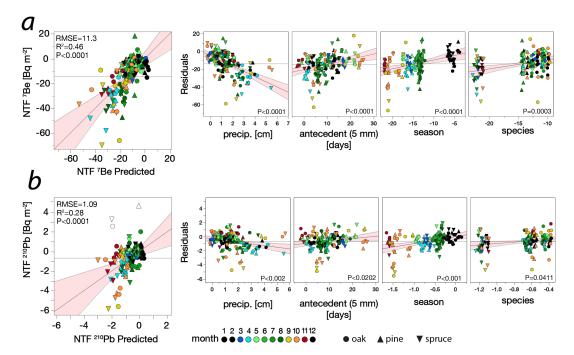


Figure 3. multiple regressions for prediction of net throughfall (NTF) of FRNs.

(a) ⁷Be and (b) ²¹⁰Pb. NTF is modeled with explanators including precipitation depth, antecedent dry period (since 5 mm precipitation), season, and tree species. Models are shown without transformation to retain interpretable units on the data but this does not impact significance of explanators. Three outliers omitted in ²¹⁰Pb regression are indicated with open symbols.

3.5. Importance of DOC and FPOM in MTE multiple regressions

For MTEs we similarly estimated dry deposition and canopy interactions that contribute to enrichments in throughfall using multiple regression. All MTEs were found to have positive correlations with both antecedent dry period and rainfall depth (Table S1). Importantly, both FPOM and DOC contribute significantly to models for all FRNs and MTEs. This suggests that carbon plays a significant role in release of both FRNs and MTEs from the canopy. DOC is the stronger explanator and typically supersedes FPOM in the model (Table S1). Because they have strong predictive power in FRN and MTE models, we also examined FPOM and DOC using multiple regression (Fig. S4). The FPOM model [R^2 =0.35] has significant explanators including season [19%], antecedent duration [11%], and rainfall depth [5%]. Surprisingly, there was no effect from species [p>0.05]. The strongest effect from antecedent duration uses a 15 mm rather than 5 mm precipitation threshold. Including DOC as an explanator strengthens the FPOM model [R^2 =0.58] as DOC becomes the strongest predictor [21%]. A model for DOC [R^2 =0.31] shows the same explanators as for FPOM, with season [14%], antecedent [7%], and rainfall depth [6%] each significant. DOC production is higher relative to FPOM in spring and fall [p<0.05], which is consistent with tree phenology and peak DOC production with both new foliar growth and senescence (Van Stan et al., 2012).

3.6. Dissolved Organic Carbon regulates FRN and MTE Net Throughfall

The coefficient θ_{DOC} obtained from multiple regression mass balance quantifies the increase in NTF per increase in DOC (μ mol-MTE μ mol-C⁻¹). This provides an empirical metric of FRN or MTE affinity for



444

445

446

447

448

449 450

451

452

453 454

455 456

457

458

459 460

461

462

464

465

466 467

468

469

470



throughfall DOC (Table S1). It can be expressed as an association constant (K_{DOC}) by normalizing each multiple regression coefficient by the average dissolved FRN or MTE concentration (μ mol L⁻¹). K_{DOC} is significantly correlated with EF across all elements, which supports the notion that DOC aids in regulating export of MTEs from the canopy (Fig. 4; R²=0.32, p=0.003; see also Hou et al., 2005 and Gandois et al., 2010). Moreover, there are additional noteworthy associations within the FRNs and MTEs. They are bound at lower EFs by group (1) consisting of ⁷Be, ²¹⁰Pb, Be^T, Pb^T, Hg^T, Al, and Fe [slope =0.381 ±0.056; R²=0.90, p=0.001]; these are elements with strongest oxide-over-humate preferences, and thus likely to be most weakly solubilized by DOC (Takahashi et al., 1999).

Separation of FRNs from their stable isotope counterparts within this relationship, with both lower K_{DOC} and lower EF, suggests that some age-dependence of PM regulates the metal-DOC association (Discussion S2, Fig. S7). Within the ⁷Be-Be^T and ²¹⁰Pb-Pb^T pairs elemental chemistry is conserved, and differences in K_{DOC} and EF must be attributed to different PM ages/sources. The distinction made here is between secondary aerosol that characterizes ⁷Be and ²¹⁰Pb and resuspended dust or aged PM that more likely influences Be^T, Pb^T, (as well as Hg^T, Al, Fe, and U). Elsewhere we have described this as a particle-age effect to describe how PM metals become increasingly and irreversibly particulate-bound with increasing PM age (Landis et al., 2021b).

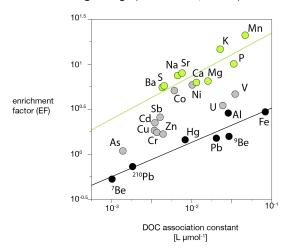


Figure 4. Dependence of throughfall EF on DOC binding constant, K_{DOC} . K_{DOC} was estimated as the increase in metal NTF per unit increase in DOC, normalized to metal concentration.

Elements in black have large oxide (K_{OH}) over oxalate binding constants (K_{OX}), elements in green have oxalate

463 preference (Takahashi et al., 1999).

> Alkaline and strongly cycled nutrient elements form a second boundary of group (2) elements at high EFs [slope =0.478 ±0.133; R²=0.72, p=0.0159]. The alkaline elements Ca, Sr and Ba have highest preference for humate over oxide ligands (Takahashi et al., 1999). K_{DOC} alone does not clearly separate groups 1 and 2 due, in part, to the particle age effect. This suggests that EF distinguishes metal source, with atmospheric deposition controlling group 1 and leaching controlling group 2. Trace metals in intermediate group (3) are increasingly likely to have metabolic contributions from canopy leaching with larger EFs.





3.7. PM storage, and change in storage, in the forest canopy

Our assumptions for FRN canopy mass balance underlying the derivation of Eq. 10 appear to be observed, with no detected differences in 7 Be and 210 Pb geochemical behaviors or rates of dry deposition. Lower 7 Be: 210 Pb ratios and excess of 210 Pb over 7 Be in TF should thus be interpreted as a change in storage (Δ S) derived from within the non-metabolic materials of the canopy. 210 Pb $_{\Delta S}$ averaged 0.70 Bq m⁻² per storm or 29% of annual net throughfall flux. In contrast to net throughfall (210 Pb $_{NTF}$) which decreases with total precipitation, 210 Pb $_{\Delta S}$ increases significantly with total precipitation at a rate of 0.22 ± 0.04 Bq m⁻² cm⁻¹, which is equivalent to 22 ± 4 Bq m⁻² per year [R²=0.19, p<0.0001]. 210 Pb $_{\Delta S}$ was not influenced by antecedent dry period [r²=0.009, p=0.25], which lends confidence that 210 Pb $_{\Delta S}$ does not simply reflect different depositional dynamics for 7 Be and 210 Pb. Multiple regression for 210 Pb $_{\Delta S}$ yielded a strong model with significant, independent effects from rainfall depth [13%], species [9%], season [7%], and DOC [15%] [R²=0.46, n=137(8)] (Fig. 5). 210 Pb $_{\Delta S}$ was highest in autumn and summer, and lowest in winter, irrespective of tree species and including the conifer species [p<0.05]. Spruce contributed larger change in storage than either pine or oak [p<0.05]. Linear, positive dependence on p_D demonstrates that 210 Pb $_{\Delta S}$ supply is not readily exhausted as is the case for dry deposition (i.e., as shown in Fig. 2a).

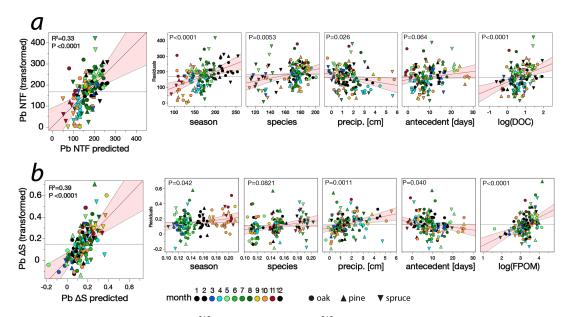


Figure 5. Multiple regressions for (a) 210 Pb net throughfall, (b) 210 Pb change in storage. Both variables are transformed to provide normal distributions.

When we compare regressions for $^{210}\text{Pb}_{\text{NTF}}$ and $^{210}\text{Pb}_{\Delta S}$, the importance of DOC is replaced by stronger correlation with FPOM in the ΔS model. In addition, where modeling of $^{210}\text{Pb}_{\text{NTF}}$ found no significant relationships with other metals, for the $^{210}\text{Pb}_{\Delta S}$ multiple regression multiple trace metals also provide explanatory power at the expense of season, DOC, and rainfall depth [R²=0.65, n=102(3)]. MTEs with strong explanatory power were $\text{Cu}_{\Delta S}$ [26%], $\text{Fe}_{\Delta S}$ [26%], $\text{Al}_{\Delta S}$ [24%], $\text{P}_{\Delta S}$ [22%] and $\text{Hg}_{\Delta S}$ [14%]. Correlation with Hg also removes autumn seasonality in $^{210}\text{Pb}_{\Delta S}$. These strong correlations among ΔS for multiple metals suggest that they are entrained in a common weathering process from the canopy. It is important to note that $^{7}\text{Be}_{\text{NTF}}$ provided no explanatory power in the $^{210}\text{Pb}_{\Delta S}$ model [p=0.35], confirming the expected decoupling of ^{7}Be and $^{210}\text{Pb}_{\Delta S}$ through the mass balance model.





- 498 Among all MTEs, ΔS increases asymptotically with EF (Fig. S5). Sulfur is a notable exception because high
- 499 EF is attributable to dry deposition of gaseous SO₂ rather than ΔS. Change in storage was estimated for
- 500 MTEs as the relative contribution to annual NTF: $SO_4 = 7\%$; $^{210}Pb = 17\%$; Cd = 40%; $^9Be = 45\%$; As = 58%;
- 501 Hg = 60%; Pb = 63%; Fe =79%; Al = 79%; P =91% (Table S1).

502 4. Discussion

503

4.1 Verifying throughfall multiple-regression mass balances

- Throughfall mass balances for the FRNs can be verified against ecosystem mass balance since, due to
- 505 their short half-lives, the FRNs measured in vegetation and soil have unambiguous atmospheric sources.
- 506 For example, long-term ²¹⁰Pb fluxes calculated from regional steady-state soil inventories average 173
- ± 24 Bg m⁻² y⁻¹ (n=8; (Landis et al., 2016, 2024b)). Long-term bulk deposition measurements average 177
- 508 ±27 (n=12) but have decreased 4% per year from 2011 to present and the most recent 4 years have
- 509 averaged 158 ±26 (Landis et al., 2021). The sum of event-based W plus D fluxes estimated from multiple
- 510 regression reported here over two years equates to 151 Bq m⁻² y⁻¹ which is somewhat lower than
- 511 expected from soil inventories. However, the multiple regression estimate of D assumes that dry
- 512 deposition is fully removed by each subsequent precipitation event (Lovett and Lindberg, 1984). Our
- analysis of throughfall FRN concentrations in storms has already shown that this is not correct (Fig. 2).
- 514 Therefore, the multiple regression approach underestimates D and thereby total annual deposition as
- well. From a whole tree mass balance approach (Landis, 2024b), an absorption rate of for *D* was
- estimated to be 53%, meaning the multiple regression underestimates D by a factor of 2. Adoption of
- 517 this absorption factor hereafter requires a proportionate increase in annual dry deposition, almost
- doubling the estimate to 65 Bq m^{-2} y^{-1} and leading to an annual deposition total of 174 Bq m^{-2} y^{-1} . This
- 519 more robust estimate with correction to rates of dry deposition stands in better agreement with soil
- 520 records. The overall conclusion we reach is that both wet and dry deposition are well retained by the
- 521 forest canopy.

532

- 522 FRNs also provide an opportunity to evaluate the suitability of conventional filtering throughfall mass
- balance for MTEs. In contrast to the multiple-regression approach, the rate of ²¹⁰Pb dry deposition
- 524 predicted by the filtering approach (Eq. 4, with Al as reference) is higher by a factor of twelve, and total
- 525 annual ²¹⁰Pb deposition is higher by a factor of two over what is observed in local soils (360 Bq m⁻² y⁻¹).
- 526 The total ⁷Be flux predicted by filtering is higher than observed by a factor of 2.6 (4700 Bg m⁻²). The
- 527 filtering approach thus grossly overestimates secondary aerosol metal deposition, irrespective of
- 528 whether Na, Al or U are used as reference elements. These elements must therefore have substantial
- 529 contributions from canopy leaching or resuspended dust that do not impact FRNs and other secondary
- 530 aerosol metals. Total rates of deposition for all MTEs estimated by the filtering approach are higher than
- the multiple-regression approach on average by a factor of 5 (*Discussion S3*).

4.2. ⁷Be:²¹⁰Pb ratios, PM age, and residence time in the phyllosphere

- 533 The strongest control on ⁷Be:²¹⁰Pb ratios in throughfall was tree species. We attribute this to an age
- 534 effect and the storage of PM in phyllosphere by conifers with high foliar masses and LAI. Decreasing
- 535 throughfall ⁷Be:²¹⁰Pb ratios in order oak > pine > spruce is consistent with characteristic leaf retention
- 536 times of each species, about 6 months for oak, 1-2 years for white pine and up to 5-8 years for spruce.
- 537 This trend is also consistent with the size of total ²¹⁰Pb inventories likely to be stored in these trees
- 538 based on whole-tree mass balance, increasing from 9-times the annual flux in oak, 11-times in pine, and
- 539 17-times the ²¹⁰Pb annual flux in spruce (Landis, 2024b). Given these large estimates of ²¹⁰Pb storage in
- 540 the canopy, and assuming that the canopy is at steady-state with respect to inputs and export, the mean
- residence time of ²¹⁰Pb storage in the canopy (S) can be described as follows, with the corresponding
- 542 analytical solution:





$$\frac{\partial S}{\partial t} = A - kS - \lambda S$$
 Eq. 15

544
$$S(t) = \frac{A}{k+\lambda} \left[1 - e^{-(k+\lambda) \cdot t} \right]$$
 Eq. 16

where *S* is canopy inventory (Bq m⁻²), *A* is the rate of canopy absorption of 210 Pb which elsewhere is estimated as the product of wet and dry fluxes with their characteristic sorption coefficients of approximately 50% each, minus litter losses, summing to 57 Bq m⁻² y⁻¹ (Landis, 2024b). Here λ is the 210 Pb decay constant, and *k* is a characteristic physicochemical weathering rate. *k* can be approximated if we observe a steady-state *S* =825 Bq m⁻² based on whole-tree measurements, which is an average for the two throughfall trees at the BM site. With these assumptions the mean residence time of aerosol metal in the phyllosphere with respect to weathering is 32 years (Fig. S6). Independent age estimates of individual components of an adjacent red oak tree have also been made with 7 Be: 210 Pb chronometry for leaves (0.5 years), twigs (1.4 years), branches (7 years), moss (28 years), lichen (21 years), live surface (20-52 years), and bark (18 to >70 years). These ages are consistent with ordering or superposition of, e.g, twig versus branch, and canopy crown versus tree base, and overall confirm that canopy storage of metals persists for decades (Landis, 2024b).

4.3. Implications for rates of MTE deposition to forest vegetation

The FRNs stand apart from MTEs in canopy mass balance, having EFs <1 and NTF that scales inversely with rainfall depth. What distinguishes the FRNs from other PM metals is radioactive decay, and the obvious cause for their diverging behaviors is a difference in characteristic ecosystem residence times. Whereas the FRNs are quintessential atmospheric metals and tracers of PM2.5, other trace metal cycles are therefore dominated by recycled pathways rather than novel PM deposition. This is illustrated clearly for the pairs ²¹⁰Pb versus Pb^T, and ⁷Be versus ⁹Be. Within each pair the FRN shows net sorption to the canopy while the stable isotope shows net release. Within each pair elemental chemistry must be conserved, and differences must therefore derive from half-life restrictions which in turn relate to different PM sources. In the absence of FRN mass balance, large EFs for both ⁹Be and Pb^T in throughfall would be attributed to novel dry deposition rather than to a change in storage from recycled materials and legacy deposition. This has obvious consequences for estimating PM budgets and dry deposition by canopy mass balance, which may otherwise be overestimated by factors ranging from 2-10 (*Discussion S3*).

A critical question thus emerges: from where does a change in storage originate? Possible sources cannot be discriminated by our current methods but include resuspension of aged particulate matter, e.g., dust, from the surrounding forest floor, as well as regional sources such as vehicular traffic and road dust; excretion of metabolic products from flora of the phyllosphere; or weathering of PM from legacy deposition to living and dead surfaces of the phyllosphere. For all MTEs, the strong dependence of both NTF and ΔS on DOC indicates that the immediate metal source is within the phyllosphere rather than surrounding ecosystem. Production of DOC in the phyllosphere in this case appears to act as a weathering mechanism, meaning that PM and dust are efficiently captured in the canopy, their constituents solubilized over some characteristic time frame that may span years to decades, likely altering their chemical speciation in association with organic carbon, and exporting them from the canopy in an operationally dissolved phase by DOC (Gandois et al., 2010; Roulier et al., 2021). Poorly soluble metals such as Fe and Al require solubilization by DOC to generate high throughfall EFs through ΔS (Hou et al., 2005). In conclusion, the strong correlations of ΔS among many TMs suggest that ΔS is an emergent ecosystem property through which metal, carbon, and hydrologic cycles converge (Van Stan and Stubbins, 2018). The phyllosphere thus plays a critical role in regulating timing, bioavailability, and reactivity of metals and carbon subsequently transferred to underlying soils.





The role of particulate matter is important in all MTE canopy cycles, as well, and warrants greater attention in future throughfall mass balance (Van Stan et al., 2021). Including the FPOM fraction in mass budgets increases the net throughfall of each MTE on average by 26%, but this number is higher for particle reactive elements including Hg (73%) or Pb (45%). Export of FPOM from the canopy mirrors processes that we observe for all MTEs. Its dependence on both precipitation and antecedent dry period, in turn, obscures the impact of these factors on MTEs which would otherwise be attributed to either leaching or novel dry deposition, respectively. Canopy FPOM export is highly seasonal, peaking strongly in summer to reflect productivity of the biological engine in the canopies of all tree species measured here (both deciduous and coniferous). The production of particulate matter via herbivory likely plays an important role in generation of FPOM (Frost and Hunter, 2004; Michalzik and Stadler, 2005). FPOM moreover figures directly in predictive models for DOC export and may thus represent a source of soluble carbon. As such, FPOM and DOC together influence trace metal cycling in the canopy and unite many trace metals in carbon cycling within the phyllosphere.

4.4. Implications of aerosol ΔS for trace metal throughfall budgets

PM storage in the forest canopy introduces complexity to metal exchange processes that control throughfall mass balance. Our compilation of literature trace metal throughfall EFs highlights the widely varying behaviors of individual metals to transit through the forest canopy, ranging from strong net sorption to strong net release. This variation is unlikely to result from elemental solubility behavior, metabolic cycling, or the vagaries of event-scale interaction between precipitation and canopy. Instead, we suggest that throughfall export from the canopy reflects the complexity of aerosol sources, how these have changed through time in both source strength and aerosol characteristics (Cho et al., 2011), and transformations that occur during PM residence both in the canopy and underlying forest soil. Thus, time and history are critical determinants in throughfall metal measurements.

With global anthropogenic emissions of many metals reduced in recent decades through emissions controls, the canopy is unlikely to be in steady-state with contemporary atmospheric deposition. Throughfall is thus likely to be a biased metric of deposition if a change in storage from prior deposition cannot be assessed. Future insights into the storage and solubilization of aerosol metals in the phyllosphere will require a combination of approaches to unravel varying sources and timescales of aerosol deposition to the canopy. Here we have shown that multiple-regression mass balance, coupled with new FRN mass balance, and in combination whole-tree measurements (Landis, 2024b), can accurately quantify both new PM deposition and release of old PM from long-term storage. We anticipate that coupling throughfall, whole-tree mass balances, and FRN chronometry with stable isotope systems of, e.g., Cd, Cu, Pb, Hg, will yield new insights into metal dynamics in forest canopies and should be a focus of future efforts to understand fate and redistribution of a atmospherically-derived metals.

623 Data Availability

The data prepared for this manuscript are freely available to the public [Landis, Joshua (2025),

"Throughfall mass balance with fallout radionuclides and major/trace elements", Mendeley Data, V1,
doi: 10.17632/r9kpgp76xh.1].

Supplementary Materials

629 Supplementary Materials supporting this manuscript are available at the publisher website.





630	Author Contributions
631	This work was completed wholly by JDL in the course of Ph.D dissertation research.
632	
633	Competing Interests
634	The author declares that no competing interests influenced the conduct or conclusions of this research.
635	
636	Acknowledgements
637	Thanks to Carl Renshaw (Dartmouth College) for constructive comments on an earlier version of this
638 639 640 641 642	manuscript. DOC was measured with assistance from Caitlin Hicks Pries (Dartmouth College). Special thanks to Brian Jackson and the Dartmouth TEA Core facility for access to QQQ-ICPMS instrumentation. Special thanks to Vivien Taylor (Dartmouth College) for assistance with Hg measurements. Radionuclide measurements were performed in the Fallout Radionuclide Analytics facility (FRNA) at Dartmouth College, www.sites.dartmouth/frna/.
638 639 640 641	manuscript. DOC was measured with assistance from Caitlin Hicks Pries (Dartmouth College). Special thanks to Brian Jackson and the Dartmouth TEA Core facility for access to QQQ-ICPMS instrumentation. Special thanks to Vivien Taylor (Dartmouth College) for assistance with Hg measurements. Radionuclide measurements were performed in the Fallout Radionuclide Analytics facility (FRNA) at Dartmouth
638 639 640 641 642	manuscript. DOC was measured with assistance from Caitlin Hicks Pries (Dartmouth College). Special thanks to Brian Jackson and the Dartmouth TEA Core facility for access to QQQ-ICPMS instrumentation. Special thanks to Vivien Taylor (Dartmouth College) for assistance with Hg measurements. Radionuclide measurements were performed in the Fallout Radionuclide Analytics facility (FRNA) at Dartmouth





- 646 References
- 647 Ali, N., Khan, E. U., Akhter, P., Rana, M. A., Rajput, M. U., Khattak, N. U., Malik, F., and Hussain, S.: Wet
- 648 depositional fluxes of 210Pb- and 7Be-bearing aerosols at two different altitude cities of North Pakistan,
- 649 Atmos Environ, 45, 5699–5709, https://doi.org/10.1016/j.atmosenv.2011.07.032, 2011.
- 650 Atteia, O. and Dambrine, É.: Dynamique d'éléments traces dans les précipitations sous le couvert de 2
- pessières peu polluées de Suisse romande, Annales des Sciences Forestières, 50, 445–459,
- 652 https://doi.org/10.1051/forest:19930503, 1993.
- 653 Avila, A. and Rodrigo, A.: Trace metal fluxes in bulk deposition, throughfall and stemflow at two evergreen
- oak stands in NE Spain subject to different exposure to the industrial environment, Atmos Environ, 38, 171–
- 655 180, https://doi.org/10.1016/j.atmosenv.2003.09.067, 2004.
- 656 Barthlott, W. and Neinhuis, C.: Purity of the sacred lotus, or escape from contamination in biological surfaces,
- 657 Planta, 202, 1-8, 1997.
- 658 Bishop, K., Shanley, J. B., Riscassi, A., de Wit, H. A., Eklöf, K., Meng, B., Mitchell, C., Osterwalder, S., Schuster,
- 659 P. F., Webster, J., and Zhu, W.: Recent advances in understanding and measurement of mercury in the
- environment: Terrestrial Hg cycling, Science of the Total Environment, 721,
- 661 https://doi.org/10.1016/j.scitotenv.2020.137647, 2020.
- 662 Böhlke, J. K. and Michel, R. L.: Contrasting residence times and fluxes of water and sulfate in two small
- 663 forested watersheds in Virginia, USA, Science of the Total Environment, 407, 4363–4377,
- 664 https://doi.org/10.1016/j.scitotenv.2009.02.007, 2009.
- 665 Bortolazzi, A., Da Ros, L., Rodeghiero, M., Tognetti, R., Tonon, G., and Ventura, M.: The canopy layer, a
- biogeochemical actor in the forest N-cycle, Science of the Total Environment, 776,
- 667 https://doi.org/10.1016/j.scitotenv.2021.146024, 2021.
- 668 Bringmark, L., Lundin, L., Augustaitis, A., Beudert, B., Dieffenbach-Fries, H., Dirnböck, T., Grabner, M. T.,
- 669 Hutchins, M., Kram, P., Lyulko, I., Ruoho-Airola, T., and Vana, M.: Trace metal budgets for forested
- 670 catchments in Europe-Pb, Cd, Hg, Cu and Zn, Water Air Soil Pollut, 224, https://doi.org/10.1007/s11270-013-
- 671 1502-8, 2013.
- 672 Chamberlain, A. C.: Interception and retention of radioactive aerosols by vegetation, Atmos Environ, 4, 57-
- 673 78, 1970.
- 674 Cho, S. H., Richmond-Bryant, J., Thornburg, J., Portzer, J., Vanderpool, R., Cavender, K., and Rice, J.: A
- 675 literature review of concentrations and size distributions of ambient airborne Pb-containing particulate
- 676 matter, Atmos Environ, 45, 5005–5015, https://doi.org/10.1016/j.atmosenv.2011.05.009, 2011.
- Demers, J. D., Driscoll, C. T., Fahey, T. J., and Yavitt, J. B.: Mercury cycling in litter and soil in different forest
- types in the Adirondack region, New York, USA, Ecological Applications, 17, 1341–1351,
- 679 https://doi.org/10.1890/06-1697.1, 2007.
- 680 Draaijers, G. P. J., Erisman, J. W., Sprangert, T., and Wyers, G. P.: The application of measurements for
- atmospheric deposition monitoring, Atmos Environ, 30, 3349–3361, 1996.
- 682 Duce, R. A., Hoffman, G. L., and Zoller, W. H.: Atmospheric Trace Metals at Remote Northern and Southern
- 683 Hemisphere Sites: Pollution or Natural?, Science (1979), 187, 60–61, 1975.
- 684 Eisalou, H. K., Şengönül, K., Gökbulak, F., Serengil, Y., and Uygur, B.: Effects of forest canopy cover and floor
- on chemical quality of water in broad leaved and coniferous forests of Istanbul, Turkey, For Ecol Manage,
- 686 289, 371–377, https://doi.org/10.1016/j.foreco.2012.10.031, 2013.





- 687 Emerson, E. W., Katich, J. M., Schwarz, J. P., McMeeking, G. R., and Farmer, D. K.: Direct Measurements of
- 688 Dry and Wet Deposition of Black Carbon Over a Grassland, Journal of Geophysical Research: Atmospheres,
- 689 123, 12,277-12,290, https://doi.org/10.1029/2018JD028954, 2018.
- 690 Emerson, E. W., Hodshire, A. L., DeBolt, H. M., Bilsback, K. R., Pierce, J. R., McMeeking, G. R., and Farmer, D.
- 691 K.: Revisiting particle dry deposition and its role in radiative effect estimates, Proc Natl Acad Sci U S A, 117,
- 692 26076–26082, https://doi.org/10.1073/pnas.2014761117, 2020.
- 693 Farmer, D. K., Boedicker, E. K., and Debolt, H. M.: Dry Deposition of Atmospheric Aerosols: Approaches,
- 694 Observations, and Mechanisms, Annu Rev Phys Chem, https://doi.org/10.1146/annurev-physchem-090519,
- 695 2021.
- 696 Farmer, J. G., Eades, L. J., Graham, M. C., Cloy, J. M., and Bacon, J. R.: A comparison of the isotopic
- 697 composition of lead in rainwater, surface vegetation and tree bark at the long-term monitoring site,
- 698 Glensaugh, Scotland, in 2007, Science of the Total Environment, 408, 3704–3710,
- 699 https://doi.org/10.1016/j.scitotenv.2010.03.050, 2010.
- 700 Forti, M. C., Bicudo, D. C., Bourotte, C., De Cicco, V., and Arcova, F. C. S.: Rainfall and throughfall chemistry in
- 701 the Atlantic Forest: a comparison between urban and natural areas (São Paulo State, Brazil), Hydrol Earth Syst
- 702 Sci, 9, 570–585, 2005.
- 703 Frost, C. J. and Hunter, M. D.: Insect canopy herbivory and frass deposition affect soil nutrient dynamics and
- 704 export in oak mesocosms, Ecology, 85, 3335-3347, https://doi.org/10.1890/04-0003, 2004.
- 705 Fu, X. W., Feng, X., Dong, Z. Q., Yin, R. S., Wang, J. X., Yang, Z. R., and Zhang, H.: Atmospheric gaseous
- 706 elemental mercury (GEM) concentrations and mercury depositions at a high-altitude mountain peak in south
- 707 China, Atmos Chem Phys, 10, 2425–2437, https://doi.org/10.5194/acp-10-2425-2010, 2010.
- 708 Gandois, L., Tipping, E., Dumat, C., and Probst, A.: Canopy influence on trace metal atmospheric inputs on
- 709 forest ecosystems: Speciation in throughfall, Atmos Environ, 44, 824–833,
- 710 https://doi.org/10.1016/j.atmosenv.2009.11.028, 2010.
- 711 Graydon, J. A., St. Louis, V. L., Hintelmann, H., Lindberg, S. E., Sandilands, K. A., Rudd, J. W. M., Kelly, C. A.,
- 712 Hall, B. D., and Mowat, L. D.: Long-term wet and dry deposition of total and methyl mercury in the remote
- 713 boreal ecoregion of Canada, Environ Sci Technol, 42, 8345–8351, https://doi.org/10.1021/es801056j, 2008.
- 714 Graydon, J. A., St. Louis, V. L., Hintelmann, H., Lindberg, S. E., Sandilands, K. A., Rudd, J. W. M., Kelly, C. A.,
- 715 Tate, M. T., Krabbenhoft, D. P., and Lehnherr, I.: Investigation of uptake and retention of atmospheric Hg(II)
- by boreal forest plants using stable Hg isotopes, Environ Sci Technol, 43, 4960–4966,
- 717 https://doi.org/10.1021/es900357s, 2009.
- 718 Grigal, D. F., Kolka, R. K., Fleck, J. A., and Nater, E. A.: Mercury budget of an upland-peatland watershed,
- 719 Biogeochemistry, 50, 95–109, https://doi.org/10.1023/A:1006322705566, 2000.
- 720 Gründel, M. and Porstendörfer, J.: Differences between the activity size distributions of the different natural
- 721 radionuclide aerosols in outdoor air, Atmos Environ, 38, 3723–3728,
- 722 https://doi.org/10.1016/j.atmosenv.2004.01.043, 2004.
- 723 Henderson, G. S., Harris, W. F., Todd, D. E., and Grizzard, T.: Quantity and Chemistry of Throughfall as
- 724 Influenced by Forest-Type and Season, Source: Journal of Ecology, 365–374 pp., 1977.
- 725 Hicks, B. B.: MEASURING DRY DEPOSITION: A RE-ASSESSMENT OF THE STATE OF THE ART, 1986.
- Hicks, B. B., Saylor, R. D., and Baker, B. D.: Journal of geophysical research, Journal of Geophysical Research:
- 727 Atmospheres, 121, 14691–14707, https://doi.org/10.1038/175238c0, 2016.





- 728 Hosker, R. P. and Lindberg, S. E.: Review: Atmospheric deposition and plant assimilation of gases and
- 729 particles, Atmospheric Environment (1967), 16, 889–910, https://doi.org/10.1016/0004-6981(82)90175-5,
- 730 1982.
- 731 Hou, H., Takamatsu, T., Koshikawa, M. K., and Hosomi, M.: Trace metals in bulk precipitation and throughfall
- in a suburban area of Japan, Atmos Environ, 39, 3583–3595,
- 733 https://doi.org/10.1016/j.atmosenv.2005.02.035, 2005.
- 734 Huang, J. H., Ilgen, G., and Matzner, E.: Fluxes and budgets of Cd, Zn, Cu, Cr and Ni in a remote forested
- 735 catchment in Germany, Biogeochemistry, 103, 59–70, https://doi.org/10.1007/s10533-010-9447-0, 2011.
- 736 IAEA: Quantification of radionuclide transfer in terrestrial and freshwater environments., IAEA-Techdoc-1616,
- 737 Vienna, 671-4 pp., https://doi.org/10.1016/j.jenvrad.2009.06.021, 2009.
- 738 IPCC: Climate Change 2021: The Physical Science Basis, International Panel on Climate Change, 3–3 pp.,
- 739 https://doi.org/10.3724/sp.j.7103161536, 2021.
- 740 Iverfeldt, Å.: Mercury in forest canopy throughfall water and its relation to atmospheric deposition, Water Air
- 741 Soil Pollut, 56, 553–564, https://doi.org/10.1007/BF00342299, 1991.
- 742 Jaenicke, R.: NATURAL AEROSOLS, Ann N Y Acad Sci, 338, 317–329, https://doi.org/10.1111/j.1749-
- 743 6632.1980.tb17129.x, 1980.
- 744 Jiskra, M., Sonke, J. E., Obrist, D., Bieser, J., Ebinghaus, R., Myhre, C. L., Pfaffhuber, K. A., Wängberg, I.,
- 745 Kyllönen, K., Worthy, D., Martin, L. G., Labuschagne, C., Mkololo, T., Ramonet, M., Magand, O., and
- 746 Dommergue, A.: A vegetation control on seasonal variations in global atmospheric mercury concentrations,
- 747 Nat Geosci, 11, 244–250, https://doi.org/10.1038/s41561-018-0078-8, 2018.
- 748 Johnson, A. H. and Siccama, T. G.: Acid deposition and forest decline, Environ Sci Technol, 17,
- 749 https://doi.org/10.1021/es00113a001, 1983.
- 750 Karwan, D. L., Siegert, C. M., Levia, D. F., Pizzuto, J., Marquard, J., Aalto, R., and Aufdenkampe, A. K.:
- 751 Beryllium-7 wet deposition variation with storm height, synoptic classification, and tree canopy state in the
- 752 mid-Atlantic USA, Hydrol Process, 30, 75–89, https://doi.org/10.1002/hyp.10571, 2016.
- 753 Karwan, D. L., Pizzuto, J. E., Aalto, R., Marquard, J., Harpold, A., Skalak, K., Benthem, A., Levia, D. F., Siegert, C.
- 754 M., and Aufdenkampe, A. K.: Direct Channel Precipitation and Storm Characteristics Influence Short-Term
- 755 Fallout Radionuclide Assessment of Sediment Source, Water Resour Res, 54, 4579-4594,
- 756 https://doi.org/10.1029/2017WR021684, 2018.
- 757 Kato, H., Onda, Y., and Gomi, T.: Interception of the Fukushima reactor accident-derived 137Cs, 134Cs and
- 758 131I by coniferous forest canopies, Geophys Res Lett, 39, 1–6, https://doi.org/10.1029/2012GL052928, 2012.
- 759 Koch, D. M., Jacob, D. J., and Graustein, W. C.: Vertical transport of tropospheric aerosols as indicated by 7Be
- 760 and 210Pb in a chemical tracer model, Journal of Geophysical Research Atmospheres, 101, 18651–18666,
- 761 https://doi.org/10.1029/96jd01176, 1996.
- 762 Kolka, R. K., Nater, E. A., Grigal, D. F., and Verry, E. S.: Atmospheric inputs of mercury and organic carbon into
- a forested upland/bog watershed, Water Air Soil Pollut, 113, 273–294,
- 764 https://doi.org/10.1023/A:1005020326683, 1999.
- 765 Kopáček, J., Turek, J., Hejzlar, J., and Šantrůčková, H.: Canopy leaching of nutrients and metals in a mountain
- 766 spruce forest, Atmos Environ, 43, 5443–5453, https://doi.org/10.1016/j.atmosenv.2009.07.031, 2009.
- 767 Laguionie, P., Roupsard, P., Maro, D., Solier, L., Rozet, M., Hébert, D., and Connan, O.: Simultaneous
- 768 quantification of the contributions of dry, washout and rainout deposition to the total deposition of particle-





- 769 bound 7Be and 210Pb on an urban catchment area on a monthly scale, J Aerosol Sci, 77, 67–84,
- 770 https://doi.org/10.1016/j.jaerosci.2014.07.008, 2014.
- 771 Lamborg, C. H., Engstrom, D. R., Fitzgerald, W. F., and Balcom, P. H.: Apportioning global and non-global
- 772 components of mercury deposition through (210)Pb indexing., Sci Total Environ, 448, 132–40,
- 773 https://doi.org/10.1016/j.scitotenv.2012.10.065, 2013.
- 774 Landis, J. D.: Age-Dating of Foliage and Soil Organic Matter: Aligning 228Th:228Ra and 7Be:210Pb
- 775 Radionuclide Chronometers over Annual to Decadal Time Scales, Environ Sci Technol, 57, 15047–15054,
- 776 https://doi.org/10.1021/acs.est.3c06012, 2023.
- 777 Landis, J. D.: Accumulation of atmospheric metals in natural vegetation, Chapter 4 in Terrestrial Exchange of
- 778 Atmospheric Metals: Insights from Fallout Radionuclides, PhD, Dartmouth College, Hanover, NH, 2024a.
- 779 Landis, J. D.: Whole-tree mass balance of fallout radionuclides and atmospheric metals, Chapter 6 in
- 780 Terrestrial Exchange of Atmospheric Metals: Insights from Fallout Radionuclides, PhD, Dartmouth College,
- 781 Hanover, 240–267 pp., 2024b.
- 782 Landis, J. D.: Throughfall mass balance with fallout radionuclides and major/trace elements, Mendeley
- 783 Data, V1, doi: 10.17632/r9kpgp76xh.1, 2025.
- 784 Landis, J. D., Renshaw, C. E., and Kaste, J. M.: Measurement of 7Be in soils and sediments by gamma
- 785 spectroscopy, Chem Geol, 291, 175–185, https://doi.org/10.1016/j.chemgeo.2011.10.007, 2012.
- 786 Landis, J. D., Renshaw, C. E., and Kaste, J. M.: Quantitative retention of atmospherically deposited elements
- 787 by native vegetation is traced by the fallout radionuclides 7Be and 210Pb, Environ Sci Technol, 48, 12022–
- 788 12030, https://doi.org/10.1021/es503351u, 2014.
- 789 Landis, J. D., Renshaw, C. E., and Kaste, J. M.: Beryllium-7 and lead-210 chronometry of modern soil
- 790 processes: The Linked Radionuclide aCcumulation model, LRC, Geochim Cosmochim Acta, 180, 109–125,
- 791 https://doi.org/10.1016/j.gca.2016.02.013, 2016.
- 792 Landis, J. D., Feng, X., Kaste, J. M., and Renshaw, C. E.: Aerosol populations, processes and ages contributing
- 793 to bulk atmospheric deposition: insights from a 9-year study of 7Be, 210Pb, sulfate and major/trace
- 794 elements, Journal of Geophysical Research: Atmospheres, 2021a.
- 795 Landis, J. D., Renshaw, C. E., and Kaste, J. M.: Sorption Behavior and Aerosol-Particulate Transitions
- of7Be,10Be, and210Pb: A Basis for Fallout Radionuclide Chronometry, Environ Sci Technol, 55, 14957–14967,
- 797 https://doi.org/10.1021/acs.est.1c03194, 2021b.
- 798 Landis, J. D., Taylor, V. F., Hintelmann, H., and Hrenchuk, L. E.: Predicting behavior and fate of atmospheric
- 799 mercury in soils: age-dating METAALICUS Hg isotope spikes with fallout radionuclide chronometry,
- 800 EnvironmentalScienceandTechnology, inprint, 2024a.
- Landis, J. D., Obrist, D., Zhou, J., Renshaw, C. E., McDowell, W. H., Nytch, C. J., Palucis, M. C., Del Vecchio, J.,
- 802 Lopez, F. M., and Taylor, V. F.: Quantifying soil accumulation of atmospheric mercury using fallout
- radionuclide chronometry, Nat Commun, 15, 5430, 2024b.
- 804 Landre, A. L., Watmough, S. A., and Dillon, P. J.: The effects of dissolved organic carbon, acidity and
- 805 seasonality on metal geochemistry within a forested catchment on the Precambrian Shield, central Ontario,
- 806 Canada, Biogeochemistry, 93, 271–289, https://doi.org/10.1007/s10533-009-9305-0, 2009.
- 807 Larssen, T., de Wit, H. A., Wiker, M., and Halse, K.: Mercury budget of a small forested boreal catchment in
- southeast Norway, Science of the Total Environment, The, 404, 290–296, 2008.





- 809 Lawson, N. M. and Mason, R. P.: Concentration of mercury, methylmercury, cadmium, lead, arsenic, and
- selenium in the rain and stream water of two contrasting watersheds in western Maryland, Water Res, 35,
- 811 4039–4052, https://doi.org/10.1016/S0043-1354(01)00140-3, 2001.
- 812 Lindberg, S. E. and Harriss, R. C.: THE ROLE OF ATMOSPHERIC DEPOSITION IN AN EASTERN U.S. DECIDUOUS
- 813 FOREST, Water Air Soil Pollut, 16, 13–31, 1981.
- 814 Lindberg, S. E., Harriss, R. C., and Turner, R. R.: Atmospheric deposition of metals to forest vegetation,
- 815 Science (1979), 216, 1609–1611, https://doi.org/10.1126/science.215.4540.1609, 1982.
- 816 Liu, H., Considine, D. B., Horowitz, L. W., Crawford, J. H., Rodriguez, J. M., Strahan, S. E., Damon, M. R.,
- 817 Steenrod, S. D., Xu, X., Kouatchou, J., Carouge, C., and Yantosca, R. M.: Using beryllium-7 to assess cross-
- tropopause transport in global models, Atmos Chem Phys, 16, 4641–4659, https://doi.org/10.5194/acp-16-
- 819 4641-2016, 2016.
- 820 St. Louis, V. L., Rudd, J. W. M., Kelly, C. A., Hall, B. D., Rolfhus, K. R., Scott, K. J., Lindberg, S. E., and Dong, W.:
- 821 Importance of the forest canopy to fluxes of methyl mercury and total mercury to boreal ecosystems, Environ
- 822 Sci Technol, 35, 3089–3098, https://doi.org/10.1021/es001924p, 2001.
- 823 St. Louis, V. L., Graydon, J. A., Lehnherr, I., Amos, H. M., Sunderland, E. M., St. Pierre, K. A., Emmerton, C. A.,
- 824 Sandilands, K., Tate, M., Steffen, A., and Humphreys, E. R.: Atmospheric concentrations and wet/dry loadings
- 825 of mercury at the remote experimental lakes area, northwestern ontario, Canada, Environ Sci Technol, 53,
- 826 8017–8026, https://doi.org/10.1021/acs.est.9b01338, 2019.
- 827 Lovett, G. M. and Lindberg, S. E.: Dry Deposition and Canopy Exchange in a Mixed Oak Forest as Determined
- 828 by Analysis of Throughfall, J Appl Ecol, 21, 1013, https://doi.org/10.2307/2405064, 1984.
- Luo, X., Bing, H., Luo, Z., Wang, Y., and Jin, L.: Impacts of atmospheric particulate matter pollution on
- 830 environmental biogeochemistry of trace metals in soil-plant system: A review, Environmental Pollution, 255,
- 831 https://doi.org/10.1016/j.envpol.2019.113138, 2019.
- 832 Mahendrappa, M. K.: Tree species and urea treatment effects on sulfur and metals in throughfall and
- 833 stemflow of some eastern Canadian forest stands, Canadian Journal of Forestry Research, 17, 1035–1042,
- 834 1987.
- 835 Mahowald, N. M., Hamilton, D. S., Mackey, K. R. M., Moore, J. K., Baker, A. R., Scanza, R. A., and Zhang, Y.:
- 836 Aerosol trace metal leaching and impacts on marine microorganisms, Nat Commun, 9,
- 837 https://doi.org/10.1038/s41467-018-04970-7, 2018.
- 838 Małek, S. and Astel, A.: Throughfall chemistry in a spruce chronosequence in southern Poland, Environmental
- 839 Pollution, 155, 517–527, https://doi.org/10.1016/j.envpol.2008.01.031, 2008.
- 840 Matschullat, J., Maenhaut, W., Zimmermann, F., and Juliane Fiebig: Aerosol and bulk deposition trends in the
- 1990's, Eastern Erzgebirge, Central Europe, Atmos Environ, 34, 3213–3221, https://doi.org/10.1016/S1352-
- 842 2310(99)00516-6, 2000.
- 843 McDowell, W. H., Pérez-Rivera, K. X., and Shaw, M. E.: Assessing the Ecological Significance of Throughfall in
- Forest Ecosystems, 299–318, https://doi.org/10.1007/978-3-030-26086-6_13, 2020.
- 845 Michalzik, B. and Stadler, B.: Importance of canopy herbivores to dissolved and particulate organic matter
- 846 fluxes to the forest floor, in: Geoderma, 227–236, https://doi.org/10.1016/j.geoderma.2004.12.006, 2005.
- 847 Michopoulos, P., Baloutsos, G., Economou, A., Nikolis, N., Bakeas, E. B., and Thomaidis, N. S.:
- Biogeochemistry of lead in an urban forest in Athens, Greece, Biogeochemistry, 73, 345–357,
- 849 https://doi.org/10.1007/s10533-004-0359-8, 2005.





- 850 Michopoulos, P., Bourletsikas, A., Kaoukis, K., Daskalakou, E., Karetsos, G., Kostakis, M., Thomaidis, N. S.,
- 851 Pasias, I. N., Kaberi, H., and Iliakis, S.: The distribution and variability of heavy metals in a mountainous fir
- forest ecosystem in two hydrological years, Global Nest Journal, 20, 188–197,
- 853 https://doi.org/10.30955/gnj.002506, 2018.
- 854 Miller, C. and Hoffman, F.: An examination of the environmental half-time for radionuclides deposited on
- 855 vegetation., Health Phys, 45, 731–744, 1983.
- 856 Obrist, D., Roy, E. M., Harrison, J. L., Kwong, C. F., William Munger, J., Moosmüller, H., Romero, C. D., Sun, S.,
- 857 Zhou, J., and Commane, R.: Previously unaccounted atmospheric mercury deposition in a midlatitude
- 858 deciduous forest, Proc Natl Acad Sci U S A, 118, https://doi.org/10.1073/pnas.2105477118, 2021.
- 859 Oziegbe, M. B., Muoghalu, J. I., and Oke, S. O.: Litterfall, precipitation and nutrient fluxes in a secondary
- lowland rain forest in Ile-Ife, Nigeria, Acta Bot Brasilica, 25, 664–671, https://doi.org/10.1590/s0102-
- 861 33062011000300020, 2011.
- 862 Petty, W. H. and Lindberg, S. E.: A intensive 1-month investigation of trace metal deposition and throughfall
- at a mountain spruce forest, Water Air Soil Pollut, 53, 213–226, 1990.
- 864 PRISM Climate Group, Oregon State University, https://prism.oregonstate.edu, data created 4 Feb 2014:
- 865 Pryor, S. C., Barthelmie, R. J., Larsen, S. E., and Sørensen, L. L.: Ultrafine particle number fluxes over and in a
- 866 deciduous forest, J Geophys Res, 122, 405–422, https://doi.org/10.1002/2016JD025854, 2017.
- 867 Rea, A. W., Lindberg, S. E., and Keeler, G. J.: Dry deposition and foliar leaching of mercury and selected trace
- 868 elements in deciduous forest throughfall, Atmos Environ, 35, 3453-3462, https://doi.org/10.1016/S1352-
- 869 2310(01)00133-9, 2001.
- 870 Rea, A. W., Lindberg, S. E., Scherbatskoy, T., and Keeler, G. J.: Mercury accumulation in foliage over time in
- two northern mixed-hardwood forests, Water Air Soil Pollut, 133, 49–67,
- 872 https://doi.org/10.1023/A:1012919731598, 2002.
- 873 Rehmus, A., Bigalke, M., Boy, J., Valarezo, C., and Wilcke, W.: Aluminum cycling in a tropical montane forest
- 874 ecosystem in southern Ecuador, Geoderma, 288, 196–203, https://doi.org/10.1016/j.geoderma.2016.11.002,
- 875 2017.
- 876 Reich, P. B., Oleksyn, J., Modrzynski, J., and Tjoelker, M. G.: Evidence that longer needle retention of spruce
- and pine populations at high elevations and high latitudes is largely a phenotypic response, Tree Physiol, 16,
- 878 643–647, https://doi.org/10.1093/treephys/16.7.643, 1996.
- 879 Resongles, E., Dietze, V., Green, D. C., Harrison, R. M., Ochoa-Gonzalez, R., Tremper, A. H., and Weiss, D. J.:
- 880 Strong evidence for the continued contribution of lead deposited during the 20th century to the atmospheric
- 881 environment in London of today, Proceedings of the National Scademy of Sciences,
- 882 https://doi.org/10.1073/pnas.2102791118/-/DCSupplemental, 2021.
- 883 Rodrigo, A., Avila, A., and Gomez-Bolea, A.: Trace metal contents in Parmelia caperata (L.) Ach. compared to
- 884 bulk deposition, throughfall and leaf-wash fluxes in two holm oak forests in Montseny (NE Spain), Atmos
- 885 Environ, 33, 359–367, 1999.
- Roulier, M., Bueno, M., Coppin, F., Nicolas, M., Thiry, Y., Rigal, F., Pannier, F., and Le Hécho, I.: Atmospheric
- 887 iodine, selenium and caesium depositions in France: II. Influence of forest canopies, Chemosphere, 273,
- 888 https://doi.org/10.1016/j.chemosphere.2020.128952, 2021.





- 889 Russell, I. J., Choquette, C. E., Fang, S., Dundulis, W. P., Pao, A. A., and Pszenny, A. A. P.: Vegetation as a Sink
- 890 for Atmospheric Particulates: Quantitative Studies in Rain and Dry Deposition tests, J Geophys Res, 86, 5347–
- 891 5363, 1981.
- 892 Saylor, R. D., Baker, B. D., Lee, P., Tong, D., Pan, L., and Hicks, B. B.: The particle dry deposition component of
- total deposition from air quality models: right, wrong or uncertain?, Tellus B Chem Phys Meteorol, 71, 1–22,
- 894 https://doi.org/10.1080/16000889.2018.1550324, 2019.
- 895 Schleppi, P., Conedera, M., Sedivy, I., and Thimonier, A.: Correcting non-linearity and slope effects in the
- 896 estimation of the leaf area index of forests from hemispherical photographs, Agric For Meteorol, 144, 236–
- 897 242, https://doi.org/10.1016/j.agrformet.2007.02.004, 2007.
- 898 Schumacher, J. C.: Stratigraphy and geochemistry of the Ammonoosuc volcanics, central Massachusetts and
- 899 southwestern New Hampshire, Am J Sci, 288, 619–663, 1988.
- 900 Schwesig, D. and Matzner, E.: Pools and fluxes of mercury and methylmercury in two forested catchments in
- 901 Germany, Science of the Total Environment, 260, 213–223, https://doi.org/10.1016/S0048-9697(00)00565-9,
- 902 2000.
- 903 Shahid, M., Dumat, C., Khalid, S., Schreck, E., Xiong, T., and Niazi, N. K.: Foliar heavy metal uptake, toxicity and
- 904 detoxification in plants: A comparison of foliar and root metal uptake, J Hazard Mater, 325, 36–58,
- 905 https://doi.org/10.1016/j.jhazmat.2016.11.063, 2017.
- 906 Shanley, J. B.: Field measurements of dry deposition to spruce foliage and petri dishes in the black forest,
- 907 F.R.G., Atmospheric Environment (1967), 23, 403–414, https://doi.org/10.1016/0004-6981(89)90586-6, 1989.
- 908 Skrivan, P., Rusek, J., Fottova, D., Burian, M., and Minarik, L.: Factors affecting the content of heavy metals in
- 909 bulk atmospheric precipitation, throughfall and stemflow in central Bohemia, Czech Republic, Water Air Soil
- 910 Pollut, 85, 841-846, 1995.
- 911 Sohrt, J., Uhlig, D., Kaiser, K., von Blanckenburg, F., Siemens, J., Seeger, S., Frick, D. A., Krüger, J., Lang, F., and
- 912 Weiler, M.: Phosphorus Fluxes in a Temperate Forested Watershed: Canopy Leaching, Runoff Sources, and In-
- 913 Stream Transformation, Frontiers in Forests and Global Change, 2, https://doi.org/10.3389/ffgc.2019.00085,
- 914 2019.
- 915 Stachurski, A. and Zimka, J. R.: Atmospheric input of elements to forest ecosystems: A method of estimation
- 916 using artificial foliage placed above rain collectors, Environmental Pollution, 110, 345–356,
- 917 https://doi.org/10.1016/S0269-7491(99)00290-0, 2000.
- 918 Staelens, J., Houle, D., De Schrijver, A., Neirynck, J., and Verheyen, K.: Calculating dry deposition and canopy
- 919 exchange with the canopy budget model: Review of assumptions and application to two deciduous forests,
- 920 Water Air Soil Pollut, 191, 149–169, https://doi.org/10.1007/s11270-008-9614-2, 2008.
- 921 Van Stan, J. T. and Pypker, T. G.: A review and evaluation of forest canopy epiphyte roles in the partitioning
- 922 and chemical alteration of precipitation, https://doi.org/10.1016/j.scitotenv.2015.07.134, 1 December 2015.
- 923 Van Stan, J. T. and Stubbins, A.: Tree-DOM: Dissolved organic matter in throughfall and stemflow, Limnol
- 924 Oceanogr Lett, 3, 199–214, https://doi.org/10.1002/lol2.10059, 2018.
- Van Stan, J. T., Levia, D. F., Inamdar, S. P., Lepori-Bui, M., and Mitchell, M. J.: The effects of phenoseason and
- 926 storm characteristics on throughfall solute washoff and leaching dynamics from a temperate deciduous
- 927 forest canopy, Science of the Total Environment, 430, 48–58,
- 928 https://doi.org/10.1016/j.scitotenv.2012.04.060, 2012.





- 929 Van Stan, J. T., Ponette-González, A. G., Swanson, T., and Weathers, K. C.: Throughfall and stemflow are
- 930 major hydrologic highways for particulate traffic through tree canopies, Front Ecol Environ, 19, 404–410,
- 931 https://doi.org/10.1002/fee.2360, 2021.
- 932 Sumerling, T. J.: The use of mosses as indicators of airborne radionuclides near a major nuclear installation,
- 933 Science of The Total Environment, 35, 22, 1984.
- 934 Takahashi, Y., Minai, Y., Ambe, S., Makide, Y., and Ambe, F.: Comparison of adsorption behavior of multiple
- 935 inorganic ions on kaolinite and silica in the presence of humic acid using the multitracer technique, Geochim
- 936 Cosmochim Acta, 63, 815–836, https://doi.org/10.1016/S0016-7037(99)00065-4, 1999.
- 937 Tan, S., Zhao, H., Yang, W., Tan, B., Yue, K., Zhang, Y., Wu, F., and Ni, X.: Forest canopy can efficiently filter
- trace metals in deposited precipitation in a subalpine spruce plantation, Forests, 10,
- 939 https://doi.org/10.3390/f10040318, 2019.
- 940 Taylor, S. R. and McLennan, S. M.: The geochemical evolution of the continental crust,
- 941 https://doi.org/10.1029/95RG00262, 1995.
- 942 Taylor, V. F., Landis, J. D., and Janssen, S. E.: Tracing the sources and depositional history of mercury to
- 943 coastal northeastern U.S. lakes, Environ Sci Process Impacts, 24, 1805–1820,
- 944 https://doi.org/10.1039/d2em00214k, 2022.
- 945 Thimonier, A., Sedivy, I., and Schleppi, P.: Estimating leaf area index in different types of mature forest stands
- 946 in Switzerland: A comparison of methods, Eur J For Res, 129, 543–562, https://doi.org/10.1007/s10342-009-
- 947 0353-8, 2010.
- 948 Ukonmaanaho, L., Starr, M., Mannio, J., and Ruoho-Airola, T.: Heavy metal budgets for two headwater
- 949 forested catchments in background areas of Finland, Environmental Pollution, 114, 63–75, 2001.
- 950 Ulrich, B.: Interaction of Forest Canopies with Atmospheric Constituents: SO2, alkali and earth alkali cations
- and chloride, in: Effects of accumulation of air pollutants in forest ecosystems, edited by: Ulrich, B. and
- 952 Pankrath, J., Spring, Dordrecht, The Netherlands, 33–45, 1983.
- 953 USEPA, U. S. E. P. A.: Human Health Risk Assessment Protocol for Hazardous Waste Combustion Facilities
- 954 Final This page deliberately left blank, EPA530-R-05-006, 2005.
- 955 Wang, X., Yuan, W., Lin, C.-J., Luo, J., Wang, F., Feng, X., Fu, X., and Liu, C.: Underestimated sink of
- 956 atmospheric mercury in a deglaciated forest chronosequence, Environ. Sci. Technol., 54, 8083–8093, 2020.
- 957 WHO: Ambient air pollution: A global assessment of exposure and burden of disease, Geneva, 2016.
- 958 WHO: WHO global air quality guidelines. Particulate matter (PM2.5 and PM10), ozone, nitrogen dioxide,
- 959 sulfur dioxide and carbon monoxide., Geneva, 2021.
- 960 Wilcke, W., Velescu, A., Leimer, S., Bigalke, M., Boy, J., and Valarezo, C.: Biological versus geochemical control
- 961 and environmental change drivers of the base metal budgets of a tropical montane forest in Ecuador during
- 962 15 years, Biogeochemistry, 136, 167–189, https://doi.org/10.1007/s10533-017-0386-x, 2017.
- 963 Winkler, R., Dietl, F., Frank, G., and Tschiersch, J.: Temporal variation of 7Be and 210Pb size distributions in
- 964 ambient aerosol, Atmos Environ, 32, 983–991, https://doi.org/10.1016/S1352-2310(97)00333-6, 1998.
- 965 Wu, Y.-L., Davidson, C. I., LIndberg, S. E., and Russell, A. G.: Resuspension of Particulate Chemical Species at
- 966 Forested Sites, Environ Sci Technol, 26, 2428–2435, https://doi.org/10.1021/es00036a014, 1992.
- 967 Wyttenbach, A. and Tobler, L.: The seasonal variation of 20 elements in 1st and 2nd year needles of Norway
- 968 spruce, Picea abies (L.) Karst, Trees, 2, 52–64, https://doi.org/10.1007/BF01196345, 1988.





Yamagata, N.: Contamination of leaves by radioactive fall-out, Nature, 198, 1220-1221, 1963. 969 970 Yamagata, N., Matsuda, S., and Chiba, M.: Radioecology of cesium-137 and strontium-90 in a forest, J Radiat 971 Res, 10, 107-112, 1969. 972 Yang, H. and Appleby, P. G.: Use of lead-210 as a novel tracer for lead (Pb) sources in plants, Sci Rep, 6, 1-9, 973 https://doi.org/10.1038/srep21707, 2016. 974 Yoshida, S. and Ichikuni, M.: Role of forest canopies in the collection and neutralization of airborne acid 975 substances, The Science of the Total Environment, 35-43 pp., 1989. 976 Zhang, S. and Liang, C.: Effect of a native forest canopy on rainfall chemistry in China's Qinling Mountains, 977 Environ Earth Sci, 67, 1503–1513, https://doi.org/10.1007/s12665-012-1594-2, 2012. 978 Zhou, J., Obrist, D., Dastoor, A., Jiskra, M., and Ryjkov, A.: Vegetation uptake of mercury and impacts on 979 global cycling, https://doi.org/10.1038/s43017-021-00146-y, 1 April 2021.